



Research Article

ISSN : 0975-7384
CODEN(USA) : JCPRC5

Gravimetric and quantum chemical studies of 1-[4-acetyl-2-(4-chlorophenyl)quinoxalin-1(4H)-yl]acetone as corrosion inhibitor for carbon steel in hydrochloric acid solution

H. Zarrok¹, A. Zarrouk^{2,*}, R. Salghi³, H. Oudda¹, B. Hammouti², M. Assouag¹, M. Taleb⁴,
M. Ebn Touhami⁵, M. Bouachrine⁶ and S. Boukhris⁷

¹Laboratoire des procédés de séparation, Faculté des Sciences, Université Ibn Tofail BP 242, 14000 Kénitra, Morocco.

²LCAE-URAC18, Faculté des Sciences, Université Mohammed I^{er} B.P. 717, 60000 Oujda, Morocco.

³Equipe de Génie de l'Environnement et de Biotechnologie, ENSA, Université Ibn Zohr, BP 1136 Agadir, Morocco.

⁴Laboratoire d'Ingénierie des Matériaux, Modélisation et Environnement (LIMME) Faculté des sciences Dhar El Mahraz Fès, Morocco.

⁵Laboratoire d'électrochimie, de corrosion et d'environnement, Faculté des Sciences, Université Ibn Tofail BP 242, 14000 Kenitra, Morocco.

⁶ESTM, University Moulay Ismail, BP 3130, Toulal, Meknès, Morocco.

⁷Equipe de Synthèse Organique, Organométallique et d'Agrochimie, Faculté des Sciences, Université Ibn Tofail, B.P. 133, 14000 Kénitra, Morocco.

ABSTRACT

1-[4-acetyl-2-(4-chlorophenyl)quinoxalin-1(4H)-yl]acetone (Q2) was examined as a corrosion inhibitor for carbon steel in 1.0 M HCl by using weight loss measurements and the quantum chemical studies using density functional theory (DFT) methods. The percentage inhibition efficiency (η), was found to increase with increase of the inhibitor concentration due to the adsorption of the inhibitor molecules on the metal surface. In addition it was established the adsorption follows Langmuir adsorption isotherm. Moreover some thermodynamic data were calculated and discussed. Quantum chemical parameters such as highest occupied molecular orbital energy (E_{HOMO}), lowest unoccupied molecular orbital energy (E_{LUMO}), energy gap (ΔE) and dipole moment (μ), the softness (σ), the fraction of the electrons transferred from the inhibitor to the metal surface (ΔN) and the total energy (TE) have been calculated for this compound. It was found that theoretical data support the experimental results.

Keywords: Carbon steel, Corrosion inhibition, HCl, Weight loss, DFT.

INTRODUCTION

The protection of metal surfaces against corrosion is an important industrial and scientific topic. Inhibitors are one of the practical mean of preventing corrosion, particularly in acidic media. Inhibitors can adhere to a metal surface to form a protective barrier against corrosive agents in contact with metal. The effectiveness of an inhibitor to provide corrosion protection depends to large extent upon the interaction between the inhibitor and the metal surface. The adsorbed inhibitors can affect the corrosion reaction either by the blocking effect of adsorbed inhibitor

on the metal surface or by the effects attributed to the change in the activation barriers of the anodic and cathodic reactions of the corrosion process.

Organic compounds which can donate electrons to unoccupied d orbitals of metal surface to form coordinate covalent bonds and can also accept free electrons from the metal surface by using their antibond orbitals to form feedback bonds constitute excellent corrosion inhibitors. Researchers conclude that the adsorption on the metal surface depends mainly on the physicochemical properties of the inhibitor group, such as the functional group, electronic density at the donor atom, p orbital character [1-20]. The molecular electronic structure with number of adsorption active centers such as S, N and O atoms, the molecular size, the mode of adsorption, the formation of metallic complexes and the projected area of the inhibitor on the metallic surface (degree of surface coverage) also affect the efficiency of inhibition.

The choice of an appropriate inhibitor depends on the physicochemical properties of the inhibitor molecule, the nature and state of the metal surface, and the type of the corrosion medium. Inhibitors have been selected mainly by using empirical knowledge based on their macroscopic physicochemical properties. Recently, the effectiveness of an inhibitor molecule has been related to its spatial as well as its electronic structure [23-26]. Quantum chemical methods are ideal tool for investigating these parameters and are able to provide an insight into the inhibitor-surface interaction. Density functional theory, which connects some traditional empirical concepts with a quantum mechanical interpretation, is very reliable in explaining the hard and soft acid-base behavior of inhibitor molecules introduced by Pearson [27-29]. The molecular structure of 1-[4-acetyl-2-(4 chlorophenyl)quinoxalin-1(4H)-yl]acetone (Q2) was shown in Fig. 1.

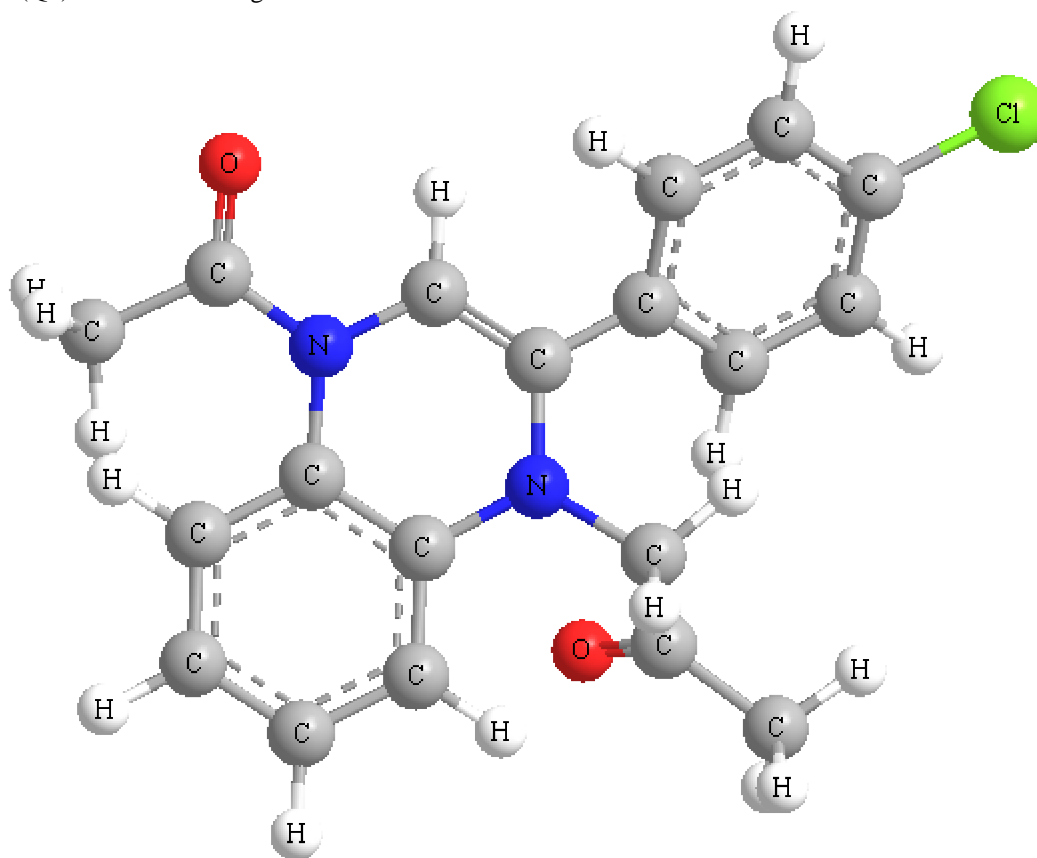


Figure 1. The chemical structure of the studied inhibitor.

The aim of this paper is to study the effect of structural parameters of 1-[4-acetyl-2-(4 chlorophenyl)quinoxalin-1(4H)-yl]acetone (Q2) on their inhibition efficiencies of corrosion of carbon steel. The inhibitory action has been investigated using weight loss measurements; the adsorption mechanism of the inhibitor on the carbon steel surface in 1.0 M HCl solution was discussed. The effect of temperature on corrosion and inhibition processes was also assessed. Theoretical calculations were further employed to explain the inhibition efficiency of Q2 as corrosion inhibitor.

EXPERIMENTAL SECTION

Materials

The steel used in this study is a carbon steel (CS) (Euronorm: C35E carbon steel and US specification: SAE 1035) with a chemical composition (in wt%) of 0.370 % C, 0.230 % Si, 0.680 % Mn, 0.016 % S, 0.077 % Cr, 0.011 % Ti, 0.059 % Ni, 0.009 % Co, 0.160 % Cu and the remainder iron (Fe).

Solutions

The aggressive solutions of 1.0 M HCl were prepared by dilution of analytical grade 37% HCl with distilled water. The concentration range of 1-[4-acetyl-2-(4 chlorophenyl)quinoxalin-1(4H)-yl]acetone (Q2) used was 10^{-6} M to 10^{-3} M.

Weight loss measurements

The carbon steel (CS) sheets of $1.6 \times 1.6 \times 0.07$ cm were abraded with a series of emery papers SiC (120, 600 and 1200) and then washed with distilled water and acetone. After weighing accurately, the specimens were immersed in a 50 mL beaker containing 80 mL 1.0 M HCl solution with and without addition of different concentrations of Q2. All the aggressive acid solutions were open to air. After 6 h the specimens were taken out, washed, dried, and weighed accurately. In order to get good reproducibility experiments were carried out in triplicate. The average weight loss of three parallel CS sheets was obtained. The tests were repeated at 308K. The corrosion rate (v) and the inhibition efficiency (η) were calculated by the following equations [30]:

$$v = \frac{W}{St} \quad (1)$$

$$\eta(\%) = \frac{v_0 - v}{v_0} \times 100 \quad (2)$$

where W is the three-experiment average weight loss of the carbon steel, S is the total surface area of the specimen, t is the immersion time and v_0 and v are values of the corrosion rate without and with addition of the inhibitor, respectively.

Computational details

Density functional theory (DFT) calculations were carried out using the Becke three-parameter nonlocal exchange functional [31] with the nonlocal correlation of Lee et al. [32] and Miehlich et al. [33], together with the standard double-zeta plus polarization 6-31G(d,p) basis set [34] implemented in the GAUSSIAN 03 program package [35]. Following the standard nomenclature the calculation will be referred to as B3LYP/6-31G*. The geometry of this compound under investigation was determined by optimizing all geometrical variables without any symmetry constraints.

According to DFT-Koopmans' theorem [36-38], the ionization potential I can be approximated as the negative of the highest occupied molecular orbital (HOMO) energy,

$$I = -E_{\text{HOMO}} \quad (3)$$

The negative of the lowest unoccupied molecular orbital (LUMO) energy is similarly related to the electron affinity A ,

$$A = -E_{\text{LUMO}} \quad (4)$$

The obtained values of I and A were considered for the calculation [29] of the electronegativity χ and the global hardness η in each of the tested molecule using the following relations:

$$\chi = \frac{I + A}{2} \quad (5)$$

$$\eta = \frac{I - A}{2} \quad (6)$$

During the interaction of the inhibitor molecule with bulk metal, electrons flow from the lower electronegativity molecule to the higher electronegativity metal until the chemical potential becomes equalized. The fraction of the transferred electron, ΔN , was estimated according to Pearson [29]

$$\Delta N = \frac{\chi_{Fe} - \chi_{inh}}{2(\eta_{Fe} + \eta_{inh})} \quad (7)$$

where a theoretical value for the electronegativity of bulk iron was used, χ (Fe) = 7 eV, and a global hardness of η (Fe) = 0 was used [39].

RESULTS AND DISCUSSION

Effect of inhibitor concentration

Table 1 displays the results obtained from the weight loss experiment after one week of carbon steel coupons immersion in 1.0 M HCl (as a function of Q2 concentration at 308K).

It can be seen that the corrosion rate decreases and inhibition efficiency increases with the inhibitor concentration. The inhibition efficiency was more than 95.8% at a concentration of 1×10^{-3} M. When the concentration of Q2 was above 1×10^{-3} M, the effect of inhibitor concentration on the inhibition efficiency was small. This indicated that the presence of inhibitor in the solution inhibits the corrosion of carbon steel by HCl and that the effectiveness of corrosion inhibition depends on the amount of Q2 present. This trend may result from the fact that both the amount of adsorption and the coverage of inhibitor on the carbon steel surface increase with inhibitor concentration. Therefore, the carbon steel surface is effectively separated from the corrosion medium by the inhibitor adsorption film [40].

Table 1 Corrosion parameters obtained from weight loss measurements for carbon steel in 1.0 M HCl containing various concentration of inhibitor at 308 K.

Inhibitor	Conc (M)	v (mg/cm ² h)	η (%)	Θ
Blank	1.0	1.070	-----	-----
Q1	1×10^{-3}	0.045	95.8	0.958
	1×10^{-4}	0.084	92.1	0.921
	1×10^{-5}	0.133	87.6	0.876
	1×10^{-6}	0.219	79.5	0.795

Effect of temperature

To investigate the mechanism of inhibition and to determine the activation energy of the corrosion process, weight loss experiments were performed in the temperature range 308-343K in the absence and presence of Q2 at 1×10^{-3} M. The corresponding data are shown in Table 2.

Table 2 Various corrosion parameters for carbon steel in 1.0 M HCl in the absence and the presence of optimum concentration of Q2 at different temperatures after 1h.

Temp (K)	Inhibitor	v (mg/cm ² h)	η %	Θ
308	Blank	1.070	-----	-----
	Q2	0.045	95.8	0.958
313	Blank	1.490	-----	-----
	Q2	0.088	94.1	0.941
323	Blank	2.870	-----	-----
	Q2	0.235	91.8	0.918
333	Blank	5.210	-----	-----
	Q2	0.761	85.4	0.854
343	Blank	10.02	-----	-----
	Q2	2.685	73.2	0.732

Table 3 represents the corrosion parameters obtained at different temperatures. Fig. 2 depicts the Arrhenius plots $\ln v$ against $1/T$ for carbon steel in 1.0 M HCl without and with the addition of 1×10^{-3} M Q2. Straight lines are obtained with very high coefficients of correlation of 0.99961 and 0.99784 for blank alone and with 1×10^{-3} M, respectively, which indicate the presence of linear relationship between $\ln v$ and $1/T$. The slopes of these straight lines allow the calculation of the Arrhenius activation energy E_a according to:

$$\ln A = \ln k - \frac{E_a}{RT} \quad (8)$$

where A is the corrosion rate, E_a is the apparent activation energy, R is the molar gas constant ($8.314 \text{ J K}^{-1} \text{ mol}^{-1}$), T is the absolute temperature, and k is the frequency factor. The fractional surface coverage θ can be easily determined from weight loss measurements by the ratio $\eta\% / 100$ if one assumes that the values of $\eta\%$ do not differ substantially from θ .

Table 3 Activation parameters for the steel dissolution in 1.0 M HCl in the absence and the presence of Q2 at optimum concentration.

Inhibitor	A ($\text{mg}/\text{cm}^2 \text{ h}$)	Linear regression coefficient (r)	E_a (kJ/mol)	ΔH_a (kJ/mol)	ΔS_a (J/mol K)
Blank	3.0066×10^9	0.99961	55.75	53.05	-72.49
Q2	4.9503×10^{15}	0.99784	100.57	97.87	46.51

The calculated E_a in the presence of $1 \times 10^{-3} \text{ M}$ Q2 ($100.57 \text{ kJ mol}^{-1}$) is almost five times higher than that obtained for the blank solution in the absence of Q2 ($55.75 \text{ kJ mol}^{-1}$). The decrease in % IE as the temperature increased and the high value of E_a in presence of Q2 can be interpreted as an indication for a physical columbic type of adsorption [41]. The high E_a in the inhibited solution can be correlated with the increased thickness of the double layer, which enhances the activation energy of the corrosion process. An alternative formulation of Arrhenius equation is given as [42]:

$$v = \frac{RT}{Nh} \exp\left(\frac{\Delta S_a}{R}\right) \exp\left(-\frac{\Delta H_a}{RT}\right) \quad (9)$$

where v is the corrosion rate, h is the Planck's constant ($6.626176 \times 10^{-34} \text{ Js}$), N is the Avogadro's number ($6.02252 \times 10^{23} \text{ mol}^{-1}$), R is the universal gas constant and T is the absolute temperature, ΔH_a the enthalpy of activation, and ΔS_a entropy of activation

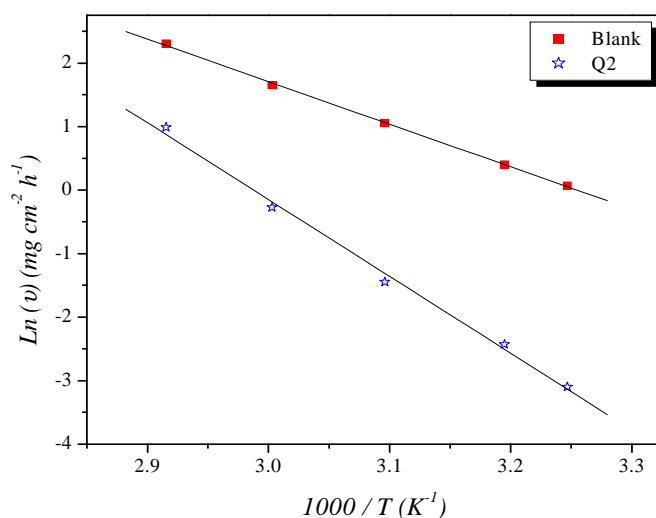


Figure 2. Arrhenius plots of $\ln v$ vs. $1/T$ for steel in 1.0 M HCl in the absence and the presence of Q2 at optimum concentration.

Fig. 3 shows a plot of $\ln(v/T)$ vs. $1/T$. Straight lines are obtained with a slope of $(-\Delta H_a/R)$ and an intercept of $[\ln(R/Nh) + (\Delta S_a/R)]$ from which the values of ΔH_a and ΔS_a are calculated and listed in Table 3. The positive sign of ΔH_a reflects the endothermic nature of the alloy dissolution process. The large negative value of ΔS_a for carbon steel in 1.0 M HCl implies that the activated complex is the rate-determining step, rather than the dissociation step. In the presence of the inhibitor, the value of ΔS_a increases and is generally interpreted as an increase in disorder as the reactants are converted to the activated complexes [43]. The positive value of ΔS_a reflect the fact that the adsorption process is accompanied by an increase in entropy, which is the driving force for the adsorption of the inhibitor onto the steel surface.

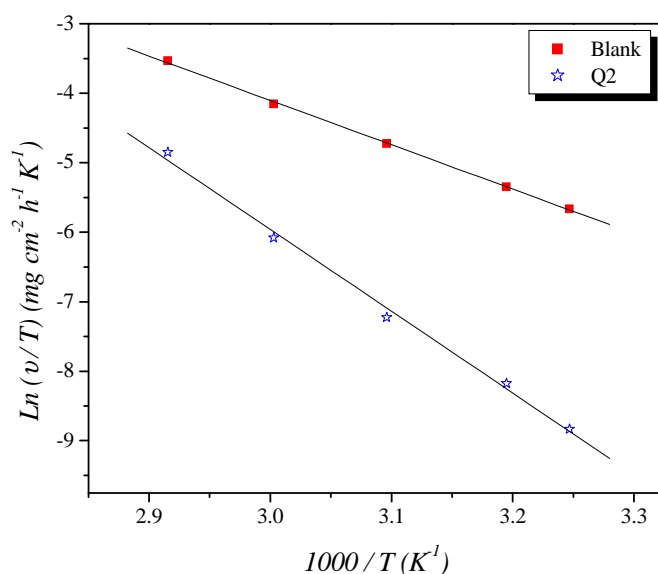


Figure 3. Arrhenius plots of $\ln(v/T)$ vs. $1/T$ for steel in 1.0 M HCl in the absence and the presence of Q2 at optimum concentration.

The adsorption isotherm

In order to investigate the adsorption mode of Q2 on the carbon steel surface that can best describe the experimental results, the degree of surface coverage (θ) for different concentrations of Q2 in 1.0 M HCl was estimated from the inhibition efficiency data ($\eta\%/100$). Several adsorption isotherms were tested with the best agreement obtained for the Langmuir adsorption isotherm [44,45]. According to this isotherm:

$$\frac{C_{\text{inh}}}{\theta} = \frac{1}{K_{\text{ads}}} + C_{\text{inh}} \quad (10)$$

with

$$K_{\text{ads}} = \left(\frac{1}{55.5}\right) \exp\left(-\frac{\Delta G_{\text{ads}}^{\circ}}{RT}\right) \quad (11)$$

where K_{ads} is the adsorption equilibrium constant, C_{inh} is the inhibitor concentration, and $\Delta G_{\text{ads}}^{\circ}$ is the standard free energy of adsorption. The value of 55.5 represents the molar concentration of water.

The agreement between the Langmuir isotherm and experimental data is very good ($R^2 = 0.99999$) where plotting C_{inh}/θ vs. C_{inh} gave a straight line with a slope of 1.0 which is very close to the theoretical value of one (Fig. 4). This suggests that the adsorption of Q2 on the carbon steel surface follows the Langmuir isotherm. The validity of Langmuir's isotherm of Q2 adsorption on carbon steel indicates that the interaction forces between the molecules in the adsorbed layer are equal to zero.

The high value of K_{ads} (565511.70 M^{-1}) reflects the increasing adsorption ability. The relatively high and negative free energy of adsorption ($\Delta G_{\text{ads}}^{\circ}$) for Q2 may indicate a relatively strong and spontaneous adsorption of Q2 on carbon steel, which explains its high corrosion inhibition efficiency. A value of -40 kJ mol^{-1} is usually adopted as a threshold value between chemical and physical adsorption [46]. The calculated value of $\Delta G_{\text{ads}}^{\circ}$, for Q2 is $-44.20 \text{ kJ mol}^{-1}$, which indicates, that the adsorption mechanism of this quinoxaline derivative on steel in 1.0 M HCl solution was typical of chemisorption.

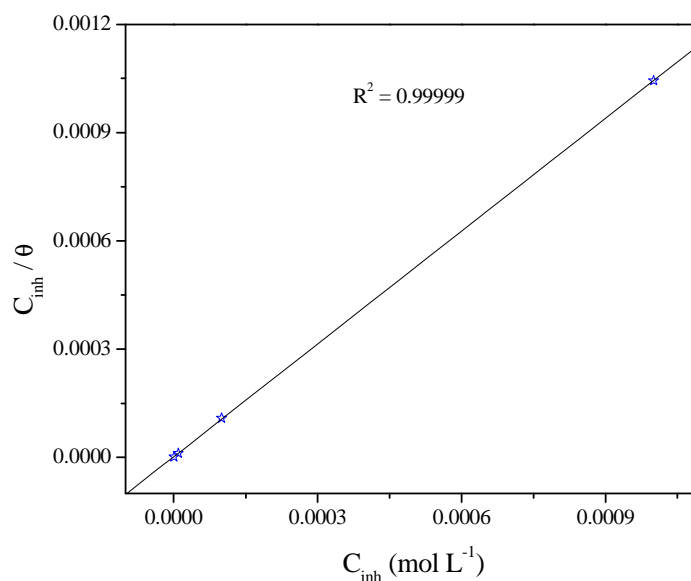


Figure 4. Langmuir adsorption of Q2 on the carbon steel surface in 1.0 HCl solution.

Quantum chemical calculation using DFT method

Density functional theory (DFT) has become very popular in recent years. This is justified based on the pragmatic observation that it is less computationally intensive than other methods with similar accuracy. This theory has been developed more recently than other ab initio methods. Because of this, there are classes of problems not yet explored with this theory, making it all the more crucial to test the accuracy of the method before applying it to unknown systems.

The premise behind DFT is that the energy of a molecule can be determined from the electron density instead of a wave function. This theory originated with a theorem by Hohenberg and Kohn that stated this was possible. The original theorem applied only to finding the ground-state electronic energy of a molecule. A practical application of this theory was developed by Kohn and Sham who formulated a method similar in structure to the Hartree-Fock method.

In this formulation, the electron density is expressed as a linear combination of basis functions similar in mathematical form to HF orbitals. A determinant is then formed from these functions, called Kohn-Sham orbitals. It is the electron density from this determinant of orbitals that is used to compute the energy.

This procedure is necessary because Fermion systems can only have electron densities that arise from an antisymmetric wave function. There has been some debate over the interpretation of Kohn-Sham orbitals. It is certain that they are not mathematically equivalent to either HF orbitals or natural orbitals from correlated calculations. However, Kohn-Sham orbitals do describe the behavior of electrons in a molecule, just as the other orbitals mentioned do. DFT orbital eigenvalues do not match the energies obtained from photoelectron spectroscopy experiments as well as HF orbital energies do. The questions still being debated are how to assign similarities and how to physically interpret the differences.

A density functional is then used to obtain the energy for the electron density. A functional is a function of a function, in this case, the electron density. The exact density functional is not known. Therefore, there is a whole list of different functionals that may have advantages or disadvantages. Some of these functionals were developed from fundamental quantum mechanics and some were developed by parameterizing functions to best reproduce experimental results. Thus, there are in essence ab initio and semiempirical versions of DFT.

DFT tends to be classified either as an ab initio method or in a class by itself.

It was shown from experimental results that it is possible to get some what better performance with Q2 as corrosion inhibitor. The electronic properties such as energy of the highest occupied molecular orbital energy (E_{HOMO}), lowest unoccupied molecular orbital energy (E_{LUMO}), energy gap (ΔE) and dipole moment (μ), the softness (σ), the fraction

of the electrons transferred from the inhibitor to the metal surface (ΔN) and the total energy (TE). The optimized molecular structures are given in Fig. 5.

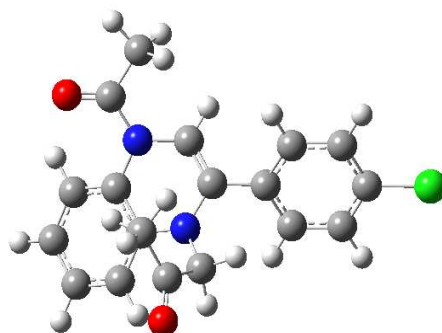


Figure 5. Optimized molecular structure of Q2.

Figure 6 shows the highest occupied molecular orbital (HOMO) and the lowest unoccupied molecular orbital (LUMO) of this molecule under study. From this figure, it can be observed that the compounds

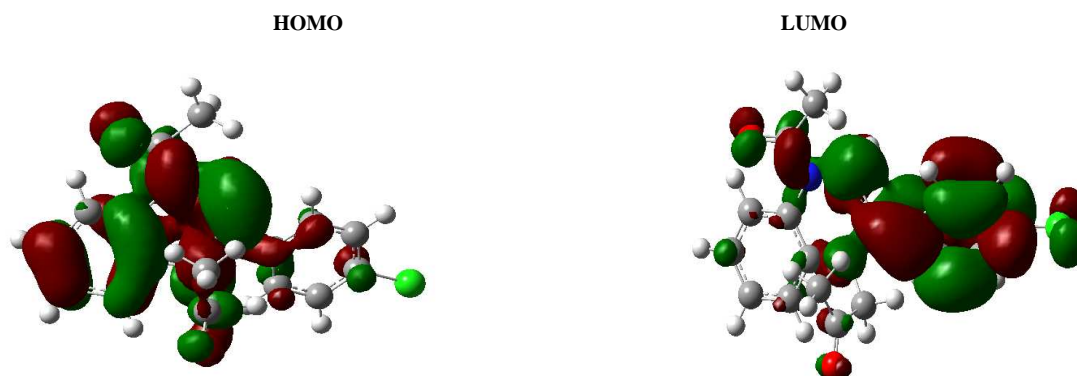


Figure 6. The obtained molecular structure, HOMO and LUMO of the neutral inhibitor molecule by *DFT/B3LYP/6-31G*(d)*.

The analysis of Figure 6 shows that the density HOMO for this compound is mainly distributed throughout the cycle quinoxaline. The LUMO density is mainly localized on the ring substituted by Cl this compound.

The calculated quantum chemical parameters for this compound are shown in Table 4. E_{HOMO} often indicates the electron donating ability of the molecule and the inhibition efficiency increases with increasing E_{HOMO} values. High E_{HOMO} values indicate that the molecule has a tendency to donate electrons to appropriate acceptor molecules with low energy empty molecular orbitals. Increasing of the values of the E_{HOMO} facilitates adsorption (and therefore inhibition) by influencing on the transport process through the adsorbed layer. The energy gap between LUMO and HOMO (ΔE) is a parameter with the smaller value causes higher inhibition efficiencies of the molecule [47,48]. In our study the highest value of $E_{\text{HOMO}} = -5.0645$ eV indicates the better inhibition efficiency. The lower value of the $E_{\text{LUMO}} = -1.28607$ eV indicates the easier of the acceptance of electrons from the d orbital of the metal. The dipole moment of Q2 is highest in the neutral form (2.666 Debye (0.87978×10^{-29} C.m)), which is higher than that of H_2O ($\mu = 6.23 \times 10^{-30}$ C.m). The high value of dipole moment probably increases the adsorption between chemical compound and metal surface [49]. Absolute hardness and softness are important properties to measure the molecular stability and reactivity. It is apparent that the chemical hardness fundamentally signifies the resistance towards the deformation or polarization of the electron cloud of the atoms, ions or molecules under small perturbation of chemical reaction. A hard molecule has a large energy gap and a soft molecule has a small energy gap [50]. In our present work the studied molecule has low hardness value 1.88921 eV and a highest value of softness of 0.52932.

The total energy calculated by quantum chemical methods is equal to -1454.4008878 eV. Hohenberg and Kohn [51] proved that the total energy of a system including that of the many body effects of electrons (exchange and correlation) in the presence of static external potential (for example, the atomic nuclei) is a unique functional of the charge density. The minimum value of the total energy functional is the ground state energy of the system. The electronic charge density which yields this minimum is then the exact single particle ground state energy.

Table 4 Some molecular properties of Q2 calculated using DFT at the B3LYP/6-31G*.

Parameters	Q2
E_{HOMO} (eV)	-5.0645
E_{LUMO} (eV)	-1.28607
ΔE_{gap} (eV)	3.778
μ (debye)	2.6660
$I = -E_{HOMO}$ (eV)	5.0645
$A = -E_{LUMO}$ (eV)	1.28607
$\chi = \frac{I + A}{2}$ (eV)	3.17528
$\eta = \frac{I - A}{2}$ (eV)	1.88921
$\sigma = \frac{1}{\eta}$	0.52932
$\Delta N = \frac{\chi_{Fe} - \chi_{inh}}{2(\eta_{Fe} + \eta_{inh})}$	1.0122538
TE (eV)	-1454.4008878

To calculate the fraction of electrons transferred, the theoretical values of χ (Fe) = 7 eV and η (Fe) = 0 are used [52]. The calculated results are presented in Table 4. Generally, value of ΔN shows inhibition efficiency resulting from electron donation, and the inhibition efficiency increases with the increase in electron-donating ability to the metal surface. Value of ΔN show inhibition effect resulted from electrons donation. According to Lukovits's study [53], if $\Delta N < 3.6$, the inhibition efficiency increases with increasing electron-donating ability at the metal surface. Based on these calculations, it is expected that the synthesized inhibitor is donor of electrons, and the steel surface is the acceptor, and this favours chemical adsorption of the inhibitor on the electrode surface. Here the inhibitor binds to the steel surface and forms an adsorption layer against corrosion. The synthesized inhibitor shows the highest inhibition efficiency because it has the highest HOMO energy and this reflects the greatest ability (the lowest ΔE) of offering electrons. It can be seen from Table 4 that the ability of the synthesized inhibitor to donate electrons to the metal surface, which is in good agreement with the higher inhibition efficiency of the synthesized inhibitor.

CONCLUSION

- The inhibition efficiency of the synthesized inhibitor increased with increasing of its concentration but it's slightly decreases with an increase in temperature range 308-343K.
 - The adsorption of Q2 on the carbon steel surface is chemical and obeyed Langmuir isotherm.
 - The calculated thermodynamic parameters such as K_{ads} and ΔG_{ads}° indicated that the Q2 adsorbed on carbon steel by a chemisorption-based mechanism.
 - The smaller gap between E_{HOMO} and E_{LUMO} favors the adsorption of Q2 on iron surface and enhancement of corrosion inhibition.
- Consequently, all results show that Q2 is a convenient inhibitor molecule against corrosion of carbon steel in HCl medium.

REFERENCES

- [1] A. K. Singh; M. A. Quraishi; *J. Mater. Environ. Sci.*, **2010**, 1, 101.
- [2] M. Prajila; J. Sam; J. Bincy; J. Abraham; *J. Mater. Environ. Sci.* **2012**, 3, 1045.
- [3] U.J. Naik; V.A. Panchal ; A.S. Patel ; N.K. Shah ; *J. Mater. Environ. Sci.*, **2012**, 3, 935.
- [4] A. Zarrouk ; H. Zarrok ; R. Salghi, B. Hammouti, F. Bentiss, R. Touri, M. Bouachrine, *J. Mater. Environ. Sci.*, **2013**, 4, 177.
- [5] H. Zarrok, H. Oudda, A. Zarrouk, R. Salghi, B. Hammouti, M. Bouachrine , *Der Pharm. Chem.*, **2011**, 3, 576.
- [6] H. Zarrok, R. Salghi, A. Zarrouk, B. Hammouti, H. Oudda, Lh. Bazzi, L. Bammou, S. S. Al-Deyab, *Der Pharm. Chem.*, **2012**, 4, 407.

- [7] H. Zarrok, S. S. Al-Deyab, A. Zarrouk, R. Salghi, B. Hammouti, H. Oudda, M. Bouachrine, F. Bentiss, *Int. J. Electrochem. Sci.*, **2012**, 7, 4047.
- [8] D. Ben Hmamou, R. Salghi, A. Zarrouk, H. Zarrok, B. Hammouti, S. S. Al-Deyab, M. Bouachrine, A. Chakir, M. Zougagh, *Int. J. Electrochem. Sci.*, **2012**, 7, 5716.
- [9] A. Zarrouk, B. Hammouti, S.S. Al-Deyab, R. Salghi, H. Zarrok, C. Jama, F. Bentiss, *Int. J. Electrochem. Sci.*, **2012**, 7, 5997.
- [10] A. Zarrouk, H. Zarrok, R. Salghi, B. Hammouti, S.S. Al-Deyab, R. Touzani, M. Bouachrine, I. Warad, T. B. Hadda, *Int. J. Electrochem. Sci.*, **2012**, 7, 6353.
- [11] A. Zarrouk, M. Messali, H. Zarrok, R. Salghi, A. Al-Sheikh Ali, B. Hammouti, S. S. Al-Deyab, F. Bentiss, *Int. J. Electrochem. Sci.*, **2012**, 7, 6998.
- [12] H. Zarrok, A. Zarrouk, R. Salghi, Y. Ramli, B. Hammouti, S. S. Al-Deyab, E. M. Essassi, H. Oudda, *Int. J. Electrochem. Sci.*, **2012**, 7, 8958.
- [13] D. Ben Hmamou, R. Salghi, A. Zarrouk, H. Zarrok, S. S. Al-Deyab, O. Benali, B. Hammouti, *Int. J. Electrochem. Sci.*, **2012**, 7, 8988.
- [14] A. Zarrouk, M. Messali, M. R. Aouad, M. Assouag, H. Zarrok, R. Salghi, B. Hammouti, A. Chetouani, *J. Chem. Pharm. Res.*, **2012**, 4, 3427.
- [15] D. Ben Hmamou, M. R. Aouad, R. Salghi, A. Zarrouk, M. Assouag, O. Benali, M. Messali, H. Zarrok, B. Hammouti, *J. Chem. Pharm. Res.*, **2012**, 4, 3489.
- [16] H. Zarrok, H. Oudda, A. El Midaoui, A. Zarrouk, B. Hammouti, M. Ebn Touhami, A. Attayibat, S. Radi, R. Touzani, *Res. Chem. Intermed* (2012) DOI 10.1007/s11164-012-0525-x
- [17] A. Zarrouk, B. Hammouti, H. Zarrok, R. Salghi, A. Dafali, Lh. Bazzi, L. Bammou, S. S. Al-Deyab, *Der Pharm. Chem.*, **2012**, 4, 337
- [18] A. Zarrouk, A. Dafali, B. Hammouti, H. Zarrok, S. Boukhris, M. Zertoubi, *Int. J. Electrochem. Sci.*, **2010**, 5, 46.
- [19] A. Zarrouk, T. Chelfi, A. Dafali, B. Hammouti, S.S. Al-Deyab, I. Warad, N. Benchat, M. Zertoubi, *Int. J. Electrochem. Sci.*, **2010**, 5, 696.
- [20] A. Zarrouk, I. Warad, B. Hammouti, A. Dafali, S.S. Al-Deyab, N. Benchat, *Int. J. Electrochem. Sci.*, **2010**, 5, 1516.
- [21] A. Zarrouk, B. Hammouti, R. Touzani, S.S. Al-Deyab, M. Zertoubi, A. Dafali, S. Elkadiri, *Int. J. Electrochem. Sci.*, **2011**, 6, 4939.
- [22] A. Zarrouk, B. Hammouti, H. Zarrok, S.S. Al-Deyab, M. Messali, *Int. J. Electrochem. Sci.*, **2011**, 6, 6261.
- [23] A.E. Stoyanova, S.D. Peyerimhoff, *Electrochim. Acta*, **2002**, 47, 1365.
- [24] L.M.R. Valdez, A.M. Villafane, D.G. Mitnik, *J. Mol. Struct.: Theochem.*, **2005**, 716, 561.
- [25] B. Gomez, N.V. Likhanova, M.A.D. Aguilar, R.M. Palou, A. Vela, J.L. Gazquez, *J. Phys. Chem. B.*, **2006**, 110, 8928.
- [26] M. Finšgar, A. Lesar, A. Kokalj, I. Milošev, *Electrochim. Acta*, **2008**, 53, 8287.
- [27] R.G. Pearson, *J. Am. Chem. Soc.*, **1963**, 85, 3533.
- [28] R.G. Pearson, *Proc. Nat. Acad. Sci.*, **1986**, 83, 8440.
- [29] G. Pearson, *Inorg. Chem.*, **1988**, 27, 734.
- [30] X.H. Li, S.D. Deng, H. Fu, G.N. Mu, N. Zhao, *Appl. Surf. Sci.*, **2008**, 254, 5574.
- [31] A.D. Becke, *J. Chem. Phys.*, **1993**, 98, 5648.
- [32] C. Lee, W. Yang, R.G. Parr, *Phys. Rev. B.*, **1988**, 37, 785.
- [33] B. Miehlich, A. Savin, H. Stoll, H. Preuss, *Chem. Phys. Lett.*, **1989**, 157, 200.
- [34] P.C. Hariharan, J.A. Pople, *Theo. Chim. Acta*, **1973**, 28, 213.
- [35] M.J. Frisch et al., GAUSSIAN 03, Revision B.03, Gaussian, Inc., Wallingford, CT, **2004**.
- [36] W.J. Hehre, L. Radom, P.v.R. Schleyer, A.J. Pople, *Ab Initio Molecular Orbital Theory*, Wiley-Interscience, New York, **1986**.
- [37] J.F. Janak, *Phys. Rev. B.*, **1978**, 18, 7165.
- [38] R. Stowasser, R. Hoffmann, *J. Am. Chem. Soc.*, **1999**, 121, 3414.
- [39] T. Arslan, F. Kandemirli, E.E. Ebenso, I. Love and H. Alemu, *Corros. Sci.*, **2009**, 51, 35.
- [40] O. Olivares-Xometl, N.V. Likhanova, M.A. Domingues-Aguilar, E. Arce, H. Dorantes, P.A. Lozada, *Mater. Chem. Phys.*, **2008**, 110, 344.
- [41] M.A. Quraishi, D. Jamal, *Mater. Chem. Phys.*, **2003**, 78, 608.
- [42] B. Hammouti, A. Zarrouk, S.S. Al-Deyab And I. Warad, *Orient. J. Chem.*, **2011**, 27, 23.
- [43] H. Zarrok, A. Zarrouk, B. Hammouti, R. Salghi, C. Jama, F. Bentiss, *Corros. Sci.*, **2012**, 64, 243.
- [44] J.H. Chun, S.K. Jeon, K.H. Ra, J.Y. Chun, *Int. J. Hydrogen Energy*, **2005**, 30, 485.
- [45] E. Khamis, *Corrosion*, **1990**, 46, 476.
- [46] E.E. Oguzie, *Corros. Sci.*, **2007**, 49, 1527.
- [47] L. Herrag, B. Hammouti, S. Elkadiri, A. Aouniti, C. Jama, H. Vezin, F. Bentiss, *Corros. Sci.*, **2010**, 52, 3042.
- [48] I.B. Obot, N.O. Obi-Egbedi, *Corros. Sci.*, **2010**, 52, 198.

- [49] X. Li, S. Deng, H. Fu, T. Li, *Electrochim. Acta*, **2009**, 54, 4089.
- [50] G. Gece, S. Bilgic, *Corros. Sci.*, **2009**, 51, 1876.
- [51] H. Ju, Z.P. Kai, Y. Li, *Corros. Sci.*, **2008**, 50, 865.
- [52] S. Martinez, *Mater. Chem. Phys.*, **2002**, 77, 97.
- [53] I. Lukovits, E. Kalman, F. Zucchi, *Corrosion*, **2001**, 57, 3.